MRI is a sensitive marker of subtle white matter pathology in hypoperfused mice

Please cite this article as: Philip R. Holland, Mark E. Bastin, Maurits A. Jansen, Gavin D. Merrifield, Robin B. Coltman, Fiona Scott, Hanna Nowers, Karim Khallout, Ian Marshall, Joanna M. Wardlaw, Ian J. Deary, James McCulloch, Karen Horsburgh, MRI is a sensitive marker of subtle white matter pathology in hypoperfused mice, *Neurobiology of Aging* (2011), DOI: 10.1016/j.neurobiolaging.2010.11.009

MRI is a sensitive marker of subtle white matter pathology in hypoperfused mice

Authors:

[1]Philip R. Holland*, [2,3,4]Mark E. Bastin, [2]Maurits A. Jansen, [2]Gavin D. Merrifield, [1]Robin B. Coltman, [1]Fiona Scott, [1]Hanna Nowers, [1]Karim Khallout, [2,3,4]Ian Marshall, [3,4]Joanna M. Wardlaw, [4]Ian J. Deary, [1]James McCulloch and [1]Karen Horsburgh*.

Authors Affiliations:

[1]Centre for Cognitive Ageing and Cognitive Epidemiology, Centre for Cognitive and Neural Systems, 1 George Square, University of Edinburgh, EH8 9JZ, United Kingdom.

[2]Medical & Radiological Sciences (Medical Physics), University of Edinburgh, United Kingdom.

[3]Scottish Imaging Network, A Platform for Scientific Collaboration (SINAPSE), Division of Clinical Neurosciences, University of Edinburgh, United Kingdom.

[4]Centre for Cognitive Ageing and Cognitive Epidemiology, Department of Psychology, University of Edinburgh, United Kingdom.

29th October 2010

Corresponding author:

*Dr Philip Holland and Dr Karen Horsburgh, Centre for Cognitive Ageing and Cognitive Epidemiology, Centre for Cognitive and Neural Systems, 1 George Square, University of Edinburgh, EH8 9JZ, United Kingdom.

Email: Philip.holland@ed.ac.uk or Karen.horsburgh@ed.ac.uk

Abstract

White matter (WM) abnormalities, possibly resulting from hypoperfusion, are key features of the aging human brain. It is unclear, however, whether *in vivo* MRI approaches, such as diffusion tensor (DT-MRI) and magnetisation transfer MRI (MT-MRI) are sufficiently sensitive to detect subtle alterations to WM integrity in mouse models developed to study the aging brain. We therefore investigated the use of DT- and MT-MRI to measure structural changes in four WM tracts following one month of moderate hypoperfusion, which results in diffuse WM pathology in C57Bl/6J mice. Following MRI, brains were processed for evaluation of white and grey matter pathology. Significant reductions in fractional anisotropy were observed in the corpus callosum ($p= 0.001$) and internal capsule ($p= 0.016$), and significant decreases in magnetisation transfer ratio in the corpus callosum ($p= 0.023$), fimbria ($p= 0.032$), internal capsule ($p= 0.046$) and optic tract ($p= 0.047$) following hypoperfusion. Hypoperfused mice demonstrated diffuse axonal and myelin pathology which was essentially absent in control mice. Both fractional anisotropy and magnetisation transfer ratio correlate with markers of myelin integrity/degradation and not axonal pathology. The study demonstrates that *in vivo* MRI is a sensitive measure of diffuse, subtle WM changes in the murine brain.

Keywords

Chronic cerebral hypoperfusion, diffusion tensor imaging, magnetisation transfer imaging and white matter.

1. Introduction

White matter (WM) lesions, a key feature of the aging brain, have predominantly been detected as hyper-intense regions on FLAIR and T2-weighted MRI. Recent advances, including diffusion tensor (DT-MRI) and magnetisation transfer MRI (MT-MRI) have been used to investigate markers of WM alterations in aging humans. DT-MRI has identified microstructural alterations in aged compared with the young brain which are not evident on routine structural MRI, specifically increased mean diffusivity (MD) and decreased fractional anisotropy (FA) (Pfefferbaum et al., 2000). DT-MRI is selectively sensitive to WM fibre bundles and relies upon the preferential diffusion of water molecules along the WM tracts rather than across them due to normal cellular architecture including axons and myelin. FA, a well characterised DT-MRI metric which indicates the fraction of the magnitude of the diffusion tensor which can be assigned to anisotropic water diffusion in each voxel, is reduced if WM architecture is disrupted (Harsan et al., 2008; Sun et al., 2005). Since the main determinant of anisotropic diffusion in WM is the dense packing of axonal membranes, with myelin playing an important but secondary role (Beaulieu 2002), FA may have increased sensitivity to axonal integrity rather than to the degree of myelination. The magnetisation transfer ratio (MTR), which measures the efficiency of magnetisation exchange between the relatively free water protons inside tissue and protons bound to macromolecules, reflects brain tissue organization and is reduced when structural damage to WM occurs, especially myelin loss (Silver et al., 1997). MTR is also reduced in normal appearing WM, as identified on T2- or FLAIR-weighted MRI, in the elderly (Silver et al., 1997), suggesting both imaging modalities have greater sensitivity to certain early changes than standard MR techniques. The inherent specificity of MT-MRI has led to its use in multiple human studies (Bastin et al., 2009; Kado et al., 2001), as well as animal models of demyelination (Harsan et al., 2008; Zaaraoui et al., 2008). Following the initial identification of altered WM structure in aging, several groups have described age-related changes in imaging biomarkers, both in normal appearing and disrupted WM (e.g. Bastin et al., 2009; Murray et al., 2005), which correlate with cognitive decline (e.g. Deary et al., 2006; Penke et al., 2010).

With the development of animal models that may mimic certain aspects of the aging brain it is crucial that imaging modalities are adapted to allow sufficient resolution to monitor disease

progression non-invasively, especially given the lack of pathological validation of MRI approaches in human studies. To date, imaging approaches have demonstrated sensitivity to severe alterations in WM structural integrity in mice, utilising varied interventions (Harsan et al., 2008; Sun et al., 2005). In mouse models of Alzheimer's disease an age dependent disruption as measured by DT-MRI has been shown (Song et al., 2004). However, no compelling *in vivo* evaluation of WM changes with normal aging has yet been carried out in rodents. Furthermore, the sensitivity of MD, FA and MTR to detect diffuse WM disruption in murine models relevant to the aging human brain remains unclear. We, and others, have therefore developed a mouse model in which anatomically diffuse histopathological alterations in WM occur in response to placement of microcoils around both common carotid arteries. This results in luminal narrowing, which has been shown to induce mild chronic cerebral hypoperfusion (Shibata et al., 2004).

In this paper we investigated the potential sensitivity of DT- and MT-MRI acquisitions adapted from human imaging studies (Bastin et al., 2009) to evaluate diffuse WM disruption *in vivo* in the murine brain. The development of highly sensitive non-invasive imaging methodologies is of critical importance for early detection of WM structural changes, the longitudinal detection of diffuse pathologies and their progression over time. The model of hypoperfusion, induced by bilateral carotid stenosis, is ideal to investigate early changes in WM integrity which may mimic certain aspects of the aging process.

2. Materials and Methods

Surgery. Male wild type C57Bl/6J mice (25-30 g) were anaesthetised with 5% isoflurane, followed by 1.2 to 1.6% in oxygen enriched air. Chronic cerebral hypoperfusion was induced as previously described (Shibata et al., 2004; see Supplementary Methods) by introducing wire microcoils (Sawane Spring Co, Japan) with an internal diameter of 0.18 mm around both common carotid arteries (n=15 mice) to induce luminal narrowing. To minimise cerebral blood flow changes as a result of coil placement a 30 min rest period was given between coils. Sham animals underwent identical surgical interventions with the omission of coil placement (n=8 mice).

Magnetic Resonance Imaging. Following 1 month recovery mice were re-anaesthetised and placed in a MRI compatible holder (Rapid Biomedical GmbH, Würzburg, Germany). Rectal temperature and respiration was monitored and controlled throughout to ensure normal physiological parameters. MRI data were collected using a Varian 7T preclinical scanner (Varian Inc., Yarnton, UK), with a 72 mm volume coil and a phased array mouse brain coil (Rapid Biomedical). The DT-MRI protocol consisted of 10 T2-weighted and sets of diffusion-weighted (b=1000 s/mm^2) axial fast spin-echo volumes acquired with diffusion gradients applied in 60 non-collinear directions, that is a total of 70 volumes (Jones et al., 1999; see Supplementary Methods). Fifteen contiguous slice locations were imaged with a field-of-view of 19.5×19.5 mm, an acquisition matrix of 96×96 (zero filled to 128×128) and slice thickness of 0.8 mm; giving an acquisition voxel dimension of 0.2×0.2×0.8 mm. The repetition (TR) and echo (TE) times for each fast spin-echo volume were 2000 and 35 ms. The MT-MRI protocol employed two spin-echo sequences (TR 2300 and TE 11.9 ms) with the same acquisition parameters as above; one acquired with a sinc-shaped magnetization transfer pulse with flip angle of 900° and duration 8.2 ms, applied 3 kHz off water resonance. MD, FA and MTR volumes were generated using 'in house' custom software and processed for region of interest (ROI) analysis using ImageJ. WM ROI (Figure 1A) including the corpus callosum, fimbria, internal capsule and optic tract were selected from T2-weighted structural volumes by an observer (PRH) blinded to surgical intervention and transferred onto the parametric maps (Figure 1B-D) for measurement.

Pathological assessment of white matter integrity. Mice were transcardialy perfused under deep anaesthesia with 4% parafomaldehyde, brains removed and paraffin embedded. Sections were cut at 6µm, and stained with haematoxylin and eosin to determine the presence of ischemic neuronal perikaryal damage. Sections corresponding to 1.4 to 1.7 mm from bregma (Figure 1A) were immunostained using standard methods. Antibodies were selected to visualise the different cellular components of WM fibre bundles and assessed blind to intervention. Loss of myelin integrity was assessed using anti-myelin-associated glycoprotein (MAG) and characterised as the presence of disorganised WM fibres and myelin debris graded on a scale (see Supplementary Methods) ranging from 0 (none) to 3 (extensive). Degraded myelin was assessed using anti-degraded myelin basic

protein (dMBP) and identified by the presence of intensely stained irregular myelin sheaths which were graded from 0 (none) to 3 (extensive). Axonal damage was assessed with anti-amyloid precursor protein (APP) and graded from 0 to 3 based on the presence of intense APP immuno-reactivity in swollen or bulbous axons. Cellular changes were assessed in all four WM tracts corresponding to the ROI used for MRI and grading summed to give a total score per animal.

Statistical analysis. MRI data is presented as the average ROI value of bilateral WM tracts for each subject and expressed as mean ± SE. Statistical comparisons of MD, FA and MTR values between hypoperfused and sham groups were carried out using a MANOVA to correct for Type 1 error. Pathological data are expressed as the sum of all WM tracts studied and analysed using the Fisher's exact test with significance set at $p< 0.05$. Correlation analysis between the grading of myelin and axonal damage and the imaging biomarkers (FA, MTR) were assessed using Spearman's rank correlation coefficient (ρ), with significance set at $p< 0.05$ (SPSS 14.0; SPSS Inc, Chicago, Ill, USA).

3. Results

Histopathology. There was no ischemic neuronal perikarya damage in any of the sham operated mice and the majority of hypoperfused mice (Figure 2A), except for two of the latter which were omitted from the study and thus all final analyses were conducted in the absence of ischaemic neuronal damage. In the sham operated mice there was minimal damage to WM in all regions studied (Figure 2B-G). Hypoperfused mice demonstrated diffuse damage to multiple WM fibre tracts. There was a significant increase in axonal damage (APP, $p= 0.04$; Figure 2B/E), myelin damage (dMBP, $p= 0.01$; Figure 2C/F) and a loss of myelin integrity (MAG, $p= 0.035$; Figure 2D/G) when compared to sham animals. However there was more extensive damage to myelin as compared to axons in response to hypoperfusion (Figure 2). Intra- (3 individual days) and inter-observer repeatability of the myelin and axonal damage grading scales demonstrated excellent reproducibility with kappa ≥ 0.827.

Magnetic Resonance Imaging. The T2-weighted imaging data revealed no overt structural changes in any of the mice studied. The Hotelling's Trace multivariate test of overall differences among groups was statistically significant for the corpus callosum ($p= 0.009$), internal capsule ($p= 0.005$) and

optic tract (p= 0.013), but not the fimbria (p= 0.218). Follow-up univariate post-hoc comparisons using the F statistic (Figure 1E) showed that FA was significantly reduced in the corpus callosum and internal capsule of hypoperfused mice, while MTR was significantly reduced in the corpus callosum, internal capsule, optic tract and fimbria when compared to sham operated animals. There was no significant change in FA between experimental and control subjects in the fimbria and optic tract and no significant difference between groups for MD in any region studied. There was a significant negative correlation between FA and pathological assessment of myelin integrity (MAG; Figure 2D) in the corpus callosum (ρ= -0.461, p= 0.04) and internal capsule (ρ= -0.646, p= 0.002). There was also a negative correlation between MTR and pathological assessment of degraded myelin (dMBP; Figure 2C) in the corpus callosum (ρ= -0.447, p= 0.047) and additionally with myelin integrity (MAG) in the internal capsule (ρ= -0.512, p= 0.021). There was no correlation between pathological assessment of axonal pathology and MRI measures studied.

4. Discussion

Our results demonstrate that *in vivo* DT- and MT-MRI imaging biomarkers are sufficiently sensitive to detect diffuse WM alterations in the murine brain. Both FA and MTR are sensitive to the subtle pathological WM changes seen in the absence of severe focal disruptions. The model utilised here results in subtle myelin pathology with only mild axonal disruption; in agreement both FA and MTR correlated with markers of myelin integrity/degradation and not axonal pathology. Due to the limited axonal pathology in this model the differences observed are likely myelin specific. Given the underlying potentially increased sensitivity of FA to axonal disruption compared to MTR, this may explain partly why FA is only significantly reduced in two of the larger WM tracts. Interestingly, MD did not show any significant differences, despite its sensitivity to subtle changes in WM structure produced by factors such as hypertension in the human brain (MacLullich, et. al., 2009). The development of highly sensitive imaging biomarkers is critically important to monitor disease progression, especially with the availability of transgenic models. To date the majority of *in vivo* MRI studies have focussed on severe focal pathologies (Harsan et al., 2007; Sun et al., 2005; Zaaraoui et

al., 2008). While it is clear that FA and MTR detect these overt focal pathologies, we have now demonstrated that they are also capable of detecting more subtle and diffuse microstructural changes in a model which may mimic certain aspects of age-related WM alterations. The observed reductions in FA (~10-14%) measured in this model are lower than those seen (~20-30%) in previous studies with a more overt pathology, which may be due to the limited axonal damage produced in this model (Harsan et al., 2007; Sun et al., 2005). Similarly MTR significantly decreased by up to 10% in our study which is much lower than observed in more severe demyelinating models (Zaaraoui et al., 2008), indicating a more subtle disruption of WM in hypoperfused mice at 1 month in agreement with the pathological findings of mild axonal damage and moderate myelin disruption. The data are in agreement with previous studies (Coltman et al., 2010; Shibata et al., 2004) demonstrating selective diffuse WM damage as a consequence of carotid microcoil application; however the association of carotid stenosis and WM disease on MRI in humans remains unclear (Adachi et al., 1997). Both are common and increase with age, raising the possibility of an association with other factors such as hypertension.

The model used in this study may also have important implications for other age related disorders such as small vessel disease. It is likely that the subtle changes observed with no obvious vascular alterations following 1 month of carotid stenosis are early responses to relatively acute interventions. It will be interesting to track pathological progression over longer time frames modelling a more prolonged hypoperfusion, which may in turn aid in our understanding of the link between carotid stenosis and age related disorders such as small vessel disease. The study of hypoperfusion in isolation may also allow for the relative involvement of further risk factors such as hypertension and diabetes to be elucidated. As such, the hypoperfusion model shows features that merit further study. Our findings are strengthened by the application to the experimental model domain of imaging methods developed to study the human brain, so called “reverse translation”. Given the small sample size, the results clearly justify further investigation and repetition in larger cohorts to explore possible underlying mechanisms, such as vascular risk factors, and their relevance to human aging.

In summary, we have successfully utilised both DT- and MT-MRI to investigate WM structural changes in a mouse model of chronic cerebral hypoperfusion. These data demonstrate that translational imaging biomarkers can be used to assess subtle WM specific alterations produced in an experimental model relevant to aging, and potentially monitor disease progression.

Acknowledgements

The work was undertaken by the University of Edinburgh Centre for Cognitive Ageing and Cognitive Epidemiology, part of the cross council Lifelong Health and Wellbeing Initiative. The authors gratefully acknowledge the support of Age UK for ‘The Disconnected Mind’ project and Lloyd's TSB Foundation Scotland/Royal Society of Edinburgh.

Disclosure statement

a) All authors certify that they do not have any actual or potential conflicts of interest, including any financial, personal or other relationships with other people or organizations within 3 years of beginning this work that could inappropriately influence (bias) this work.

b) All experiments were performed under an appropriate Home Office Licence with the approval of the University of Edinburgh Ethical Review Panel and subject to the Animals (Scientific Procedures) Act 1986.

References

Adachi, T., Takagi, M., Hoshino, H., Inafuku, T. 1997. Effect of extracranial carotid artery stenosis and other risk factors for stroke on periventricular hyperintensity. Stroke 28(11), 2174-2179.

Bastin, M.E., Clayden, J.D., Pattie, A., Gerrish, I.F., Wardlaw, J.M., Deary, I.J. 2009. Diffusion tensor and magnetization transfer MRI measurements of periventricular white matter hyperintensities in old age. Neurobiol. Aging 30(1), 125-136.

Beaulieu, C. 2002. The basis of anisotropic water diffusion in the nervous system - a technical review. NMR Biomed. 15(7-8), 435-455.

Coltman, R., Spain, A., Tsenkina, Y., Fowler, J.H., Smith, J., Scullion, G., Allerhand, M., Scott, F., Kalaria, R.N., Ihara, M., Daumas, S., Deary, I.J., Wood, E., McCulloch, J., Horsburgh, K. 2010. Selective white matter pathology induces specific impairment in spatial working memory. Neurobiol. Aging. PMID: 20961660.

Deary, I.J., Bastin, M.E., Pattie, A., Clayden, J.D., Whalley, L.J., Starr, J.M., Wardlaw, J.M. 2006. White matter integrity and cognition in childhood and old age. Neurology 66(4), 505-512.

Harsan, L.A., Poulet, P., Guignard, B., Parizel, N., Skoff, R.P., Ghandour, M.S. 2007. Astrocytic hypertrophy in dysmyelination influences the diffusion anisotropy of white matter. J. Neurosci. Res. 85(5), 935-944.

Harsan, L.A., Steibel, J., Zaremba, A., Agin, A., Sapin, R., Poulet, P., Guignard, B., Parizel, N., Grucker, D., Boehm, N., Miller, R.H., Ghandour, M.S. 2008. Recovery from chronic demyelination by thyroid hormone therapy: myelinogenesis induction and assessment by diffusion tensor magnetic resonance imaging. J. Neurosci. 28(52), 14189-14201.

Jones, D.K., Horsfield, M.A., Simmons, A. 1999. Optimal strategies for measuring diffusion in anisotropic systems by magnetic resonance imaging. Magn. Reson. Med. 42(3), 515-525.

Kado, H., Kimura, H., Tsuchida, T., Yonekura, Y., Tokime, T., Tokuriki, Y., Itoh, H. 2001. Abnormal magnetization transfer ratios in normal-appearing white matter on conventional MR images of patients with occlusive cerebrovascular disease. AJNR Am. J. Neuroradiol. 22(5), 922-927.

Murray, A.D., Staff, R.T., Shenkin, S.D., Deary, I.J., Starr, J.M., Whalley, L.J. 2005. Brain white matter hyperintensities: relative importance of vascular risk factors in nondemented elderly people. Radiology 237(1), 251-257.

Penke, L., Maniega, S.M., Houlihan, L.M., Murray, C., Gow, A.J., Clayden, J.D., Bastin, M.E., Wardlaw, J.M., Deary, I.J. 2010. White matter integrity in the splenium of the corpus callosum is related to successful cognitive aging and partly mediates the protective effect of an ancestral polymorphism in ADRB2. Behav. Genet. 40(2), 146-156.

Pfefferbaum, A., Sullivan, E.V., Hedehus, M., Lim, K.O., Adalsteinsson, E., Moseley, M. 2000. Age-related decline in brain white matter anisotropy measured with spatially corrected echo-planar diffusion tensor imaging. Magn. Reson. Med. 44(2), 259-268.

Shibata, M., Ohtani, R., Ihara, M., Tomimoto, H. 2004. White matter lesions and glial activation in a novel mouse model of chronic cerebral hypoperfusion. Stroke 35(11), 2598-2603.

Silver, N.C., Barker, G.J., MacManus, D.G., Tofts, P.S., Miller, D.H. 1997. Magnetisation transfer ratio of normal brain white matter: a normative database spanning four decades of life. J. Neurol. Neurosurg. Psychiatry 62(3), 223-228.

Song, S.K., Kim, J.H., Lin, S.J., Brendza, R.P., Holtzman, D.M. 2004. Diffusion tensor imaging detects age-dependent white matter changes in a transgenic mouse model with amyloid deposition. Neurobiol. Dis. 15(3), 640-647.

Sun, S.W., Neil, J.J., Liang, H.F., He, Y.Y., Schmidt, R.E., Hsu, C.Y., Song, S.K. 2005. Formalin fixation alters water diffusion coefficient magnitude but not anisotropy in infarcted brain. Magn. Reson. Med. 53(6), 1447-1451.

Zaaraoui, W., Deloire, M., Merle, M., Girard, C., Raffard, G., Biran, M., Inglese, M., Petry, K.G., Gonen, O., Brochet, B., Franconi, J.M., Dousset, V. 2008. Monitoring demyelination and remyelination by magnetization transfer imaging in the mouse brain at 9.4 T. MAGMA 21(5), 357-362.

Figure Legends

Figure 1. (A) Region-of-interest analysis on a T2-weighted volume, (B) representative fractional anisotropy (FA), (C) magnetisation transfer ratio (MTR) and (D) mean diffusivity (MD) parametric maps. (E) FA, MTR and MD alterations in sham and chronic cerebral hypoperfusion mice. MTR was significantly reduced in all four white matter tracts in the hypoperfused mice, whereas FA was significantly reduced in corpus callosum and internal capsule only. There was no significant change in MD in any region studied.

Figure 2. Representative images illustrating the integrity of the neuronal perikarya (A: CA1 region of the hippocampus), axonal integrity (B: APP) and myelin integrity (C: dMBP, D: MAG) in sham and hypoperfused mice. Axonal damage was significantly increased in hypoperfused mice (B/E), and degraded myelin (C/F) and loss of myelin integrity (D/G) were also significantly increased following 1 month hypoperfusion (*indicates $p < 0.05$, scale bar = 50 μm).

SUPPLEMENTARY METHODS

Animals and experimental design

All animals were maintained under standard housing conditions with food and water available ad lib and standard 12 hour light dark cycles. All procedures were carried out in accordance with the United Kingdom Animals (Scientific Procedures) Act 1986. Male wild type C57Bl/6J mice (25–30 g, 3–4 month old), a normal inbred strain of mouse which is widely used due to its permissive background which allows maximal expression of most transgenic mutations, were randomly assigned to different experimental groups. Mice were anaesthetised with 5% isoflurane, followed by 1.2 to 1.6% in oxygen enriched air. Chronic cerebral hypoperfusion was induced as previously described by introducing wire microcoils (Sawane Spring Co, Japan) with an internal diameter of 0.18 mm around both common carotid arteries (n = 15 mice) to induce luminal narrowing. To minimise cerebral blood flow changes as a result of coil placement a 30 min rest period was given between coils. Sham animals underwent identical surgical interventions with the omission of coil placement (n=8 mice). Anaesthetic level and rectal temperature were closely monitored and the mice maintained between 36.5 and 47.5°C to maintain normal physiological parameters. Mice were recovered for 1 hour in an incubation chamber and monitored closely throughout. Body weight and general health were recorded at regular intervals throughout the study.

MRI

Following 1 month recovery mice were anaesthetised with 5% isoflurane followed by 1.2-1.4% in oxygen enriched air for maintenance and placed in an MRI compatible custom mouse holder (Rapid Biomedical GmbH, Würzburg, Germany) for imaging experiments. Rectal temperature was monitored and maintained via a thermostatically controlled fan device and respiration was monitored throughout (Small Animal Instrument Inc., Stony Brook, USA) to ensure normal physiological parameters. MRI data was collected using a Varian 7T preclinical scanner (Varian Inc., Yarnton, UK) fitted with a 400 mT/m gradient set, a 72 mm diameter volume coil for RF transmission and a 2-channel phased array mouse brain coil (Rapid Biomedical GmbH) for signal reception. The DT-MRI protocol consisted of 10 T2-weighted and sets of diffusion-weighted (b=1000 s/mm^2) axial fast spin-echo volumes acquired

with diffusion gradients applied in 60 non-collinear directions, that is a total of 70 volumes (Jones, et al., 1999). Fifteen contiguous slice locations were imaged with a field-of-view of 19.5×19.5 mm, an acquisition matrix of 96×96 (zero filled to 128×128) and slice thickness of 0.8 mm; giving an acquisition voxel dimension of 0.2×0.2×0.8 mm. The repetition (TR) and echo (TE) times for each fast spin-echo volume were 2000 and 35 ms. The MT-MRI protocol employed two spin-echo sequences (TR 2300 and TE 11.9 ms) with the same acquisition parameters as above; one acquired with a sinc-shaped magnetization transfer pulse with flip angle of 900° and duration 8.2 ms, applied 3 kHz off water resonance. MD, FA and MTR volumes were generated using 'in house' custom software and processed for region-of-interest (ROI) analysis using ImageJ. WM ROI (Figure 1A) including the corpus callosum, fimbria, internal capsule and optic tract were selected from T2-weighted structural volumes by an observer (PRH) blinded to surgical intervention and transferred onto the parametric maps (Figure 1B-D) for measurement.

Pathological assessment

Following MRI mice were transcardialy perfused under deep anaesthesia (5% isoflurane in oxygen enriched air) with 20 ml of 0.9% heparinised phosphate buffered saline followed by 20 ml of 4% parafomaldehyde in 0.1% phosphate buffer. Brains were carefully removed and postfixed overnight in 4% papformaldehyde before being processed for paraffin embedding. Sections were cut at 6µm, mounted on poly-L-lysine coated slides and stained with haematoxylin and eosin to determine the presence of ischemic neuronal perikaryal damage in the hippocampus and striatum, grey matter structures which are sensitive to cerebral blood flow reductions. Adjacent sections corresponding to 1.4 to 1.7 mm from bregma (Figure 1A) were immunostained using standard methods following pre-treatment to remove paraffin, and in the case of amyloid precursor protein (APP) antigen retrieval with microwaving in 10mM citrate buffer (pH 6). Antibodies were selected to visualise the different cellular components of WM fibre bundles and assessed blind to intervention. Myelin integrity was assessed using anti-myelin-associated glycoprotein (MAG) (1:500; Santa Cruz Biotechnologies, Santa Cruz, CA, USA) and anti-degenerated myelin basic protein (dMBP) (1:300; Millipore, Billerica, MA,

USA). Axonal damage was assessed using anti APP antibody (1:1000; Millipore). Sections were incubated with primary antibody overnight at 4°C following blocking then biotinylated secondary antibodies (1:100) and a solution of streptavidinbiotin-peroxidase complex. Peroxidase activity was localised using 3,3'diaminobenzadine tetrahydrochloride as a chromagenic substrate (Vector Labs, Peterborough, UK).

The grading system which has previously demonstrated sufficient sensitivity to detect white matter disruption in this model (Coltman, et al., 2010) was conducted by an experienced individual blind to the surgical intervention. Myelin integrity with MAG was classed as the presence of disorganised white matter fibres and myelin debris with the following scale: normal (grade 0), minimal myelin debris, vacuolation and disorganisation of fibres (grade 1), modest myelin debris, vacuolation and disorganisation of fibres (grade 2), and extensive myelin debris, vacuolation and disorganisation of fibres (grade 3). Degraded myelin which is positively immunostained with dMBP was graded using the following scale: no degraded myelin present (grade 0), minimal degraded myelin (grade 1), moderate areas of degraded myelin (grade 2), and extensive areas of degraded myelin (grade 3). Axonal damage as measured by intense APP immunoreactivity in swollen or bulbous axons was graded with the following scale: normal (grade 0), minimal axonal damage (grade 1), moderate areas of axonal damage (grade 2), and extensive areas of axonal damage (grade 3). Cellular changes were assessed in all four WM tracts corresponding to the ROI used for MRI and grading summed to give a total score per animal.

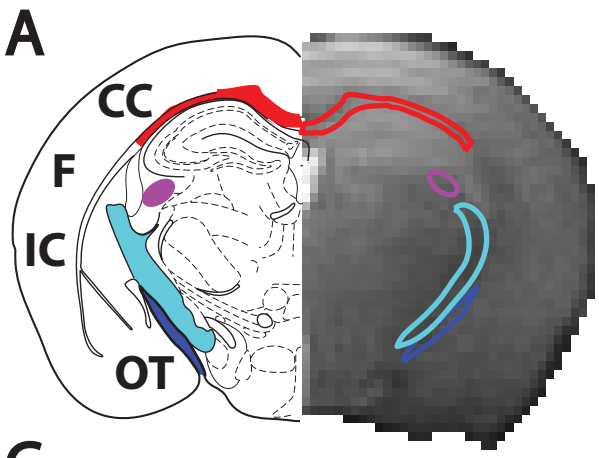

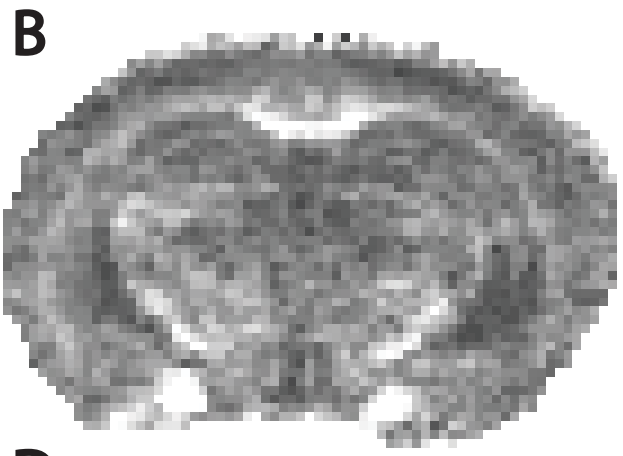

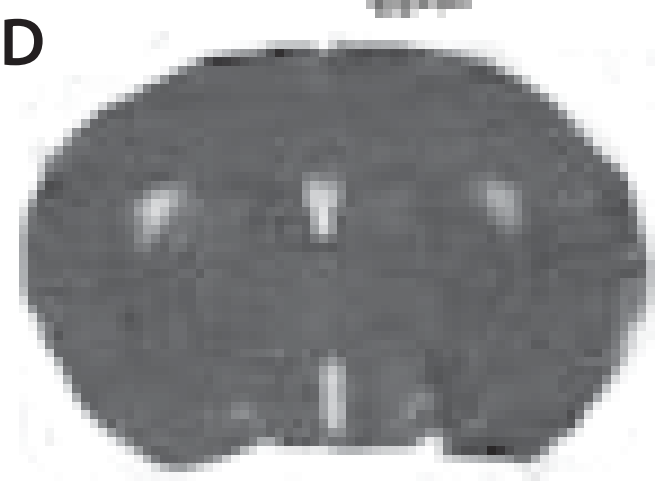

E

Region of Interest	Biomarker	Sham	Hypoperfused	Statistics	% Change
Corpus Callosum (CC)	FA	0.394 ± 0.010	0.347 ± 0.006	$F_{(1,18)}$ = 16.5, p=0.001	-13.54
	MTR	28.26 ± 0.857	25.73 ± 0.610	$F_{(1,18)}$ = 6.14, p=0.023	-9.832
	MD (x10^{-4})	6.95 ± 0.051	6.71 ± 0.021	$F_{(1,18)}$ = 6.12, p=0.444	-3.57
Internal Capsule (IC)	FA	0.392 ± 0.013	0.357 ± 0.006	$F_{(1,18)}$ = 7.06, p=0.016	-9.80
	MTR	30.32 ± 0.647	28.62 ± 0.481	$F_{(1,18)}$ = 4.58, p=0.046	-5.94
	MD (x10^{-4})	6.82 ± 0.031	6.53 ± 0.024	$F_{(1,18)}$ = 0.58, p=0.456	-4.44
Optic Tract (OT)	FA	0.403 ± 0.027	0.353 ± 0.014	$F_{(1,17)}$ = 3.34, p=0.085	-14.16
	MTR	28.33 ± 0.692	25.85 ± 0.851	$F_{(1,17)}$ = 4.60, p=0.047	-9.59
	MD (x10^{-4})	6.79 ± 0.033	6.47 ± 0.021	$F_{(1,17)}$ = 0.76, p=0.393	-4.94
Fimbria (F)	FA	0.494 ± 0.029	0.480 ± 0.025	$F_{(1,18)}$ = 0.12, p=0.731	-2.91
	MTR	28.27 ± 0.811	25.95 ± 0.608	$F_{(1,18)}$ = 5.40, p=0.032	-8.94
	MD (x10^{-4})	7.62 ± 0.029	7.5 ± 0.033	$F_{(1,18)}$ = 0.04, p=0.833	-1.6

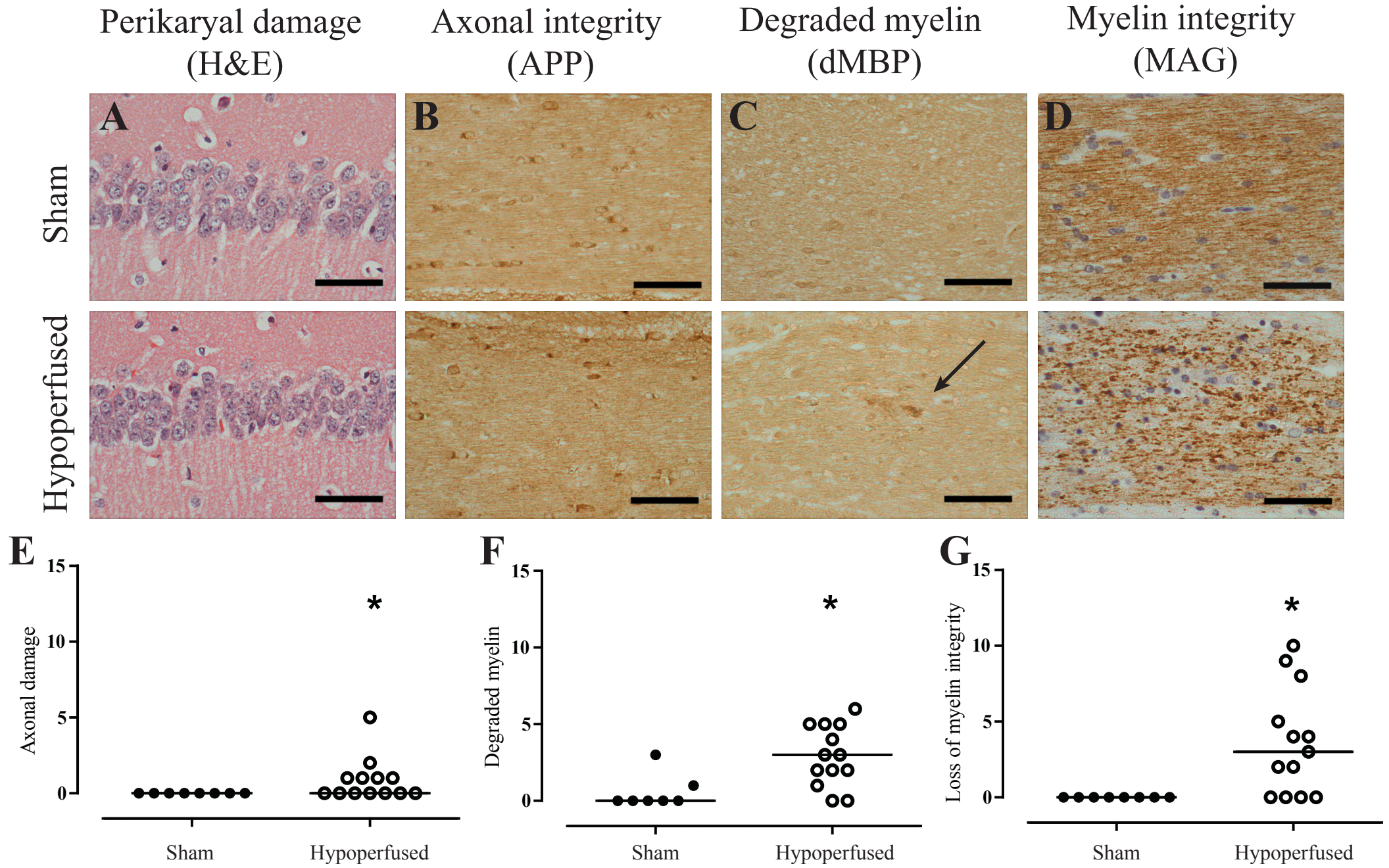

Figure 2. Holland et al.